Journal of the Meteorological Society of Japan

EARLY ONLINE RELEASE

The DOI for this manuscript is

DOI:10.2151/jmsj.2019-006

J-STAGE Advance published date: October 29th, 2018

A simple model of the resonant interaction between vortex Rossby and gravity waves

Mayuko ODA

Typhoon Depertment, Meteorological Research Institute, Tsukuba, Japan

and

Hirotada KANEHISA

Ryugasaki, Japan

October 16, 2018

Corresponding author: Mayuko Oda, Typhoon Depertment , Meteorological Research Institute , 1-1, Nagamine, Tsukuba, Ibaraki 305-0052, Japan.
E-mail: odamayuk@mri-jma.go.jp

Abstract

A simple conceptual model of the resonant interaction in a typhoon-like vortex between vortex Rossby waves (VRWs) and gravity waves (GWs), which are caused by the VRWs, is presented. It is well known that the VRWs in the central region of the vortex can grow by the interaction with the GWs in the outer region, but a simple conceptual model for their interaction has not yet been proposed. The proposed conceptual model is based on the buoyancy-vorticity formulation (BV-thinking), and is different from that for the barotropic and baroclinic instabilities based on PV interactions (PV-thinking).

We consider disturbances of the first baroclinic mode on a basic barotropic vortex. The disturbance vertical vorticity ζ of the VRW in the central region has a large amplitude on the upper and lower levels. While, the disturbance buoyancy b and radial vorticity η of the GW have a large amplitude on the middle level. The central VRW propagates (relative to the fluid) anticyclonically, but moves cyclonically because of the strong cyclonic advection by the vortex. The outer cyclonically propagating GW is weakly advected also cyclonically by the vortex. As a result, the counter-propagating VRW and GW (satisfying Rayleigh's condition) may be phase-locked with each other (satisfying Fjørtoft's condition).

By the counter-propagation and phase-lock, the circulation around ζ of

the VRW enhances b of the GW, which in turn enhances η. At the same time, the circulation around η of the GW enhances ζ of the VRW. As a result, the VRW and GW grow simultaneously.

We analytically show the possibility of the resonant interaction, and numerically obtain the growing solution in the system linearized about the basic vortex.

Keywords typhoon; vortex Rossby wave ; gravity wave

1. Introduction

On a typhoon-like axisymmetric vortex, vortex Rossby waves (VRWs) exist supported by the radial gradient of the vertical vorticity. In addition, gravity waves (GWs) also exist supported by the vertical gradient of the buoyancy which is proportional to the potential temperature. Asymmetric disturbances on a typhoon-like axisymmetirc vortex are considered to consist of VRWs and GWs. Asymmetric disturbances are known to influence the intensity and track of a typhoon. For example, Willoughby(1977, 1978) interpreted the spiral rain bands as inward-propagating GWs. Montgomery and Kallenbach (1997) interpreted them as outward-propagating VRWs, and showed that the axisymmetrization of the VRWs intensifies the axisymmetric vortex. Schubert et al. (1999), and Kossin and Schubert (2001, 2004) proposed that polygonal eyes of a typhoon are formed by VRWs with various azimuthal wave numbers in the vicinity of the eyewall. Nolan and Montgomery (2000, 2001, 2002) proposed that the meandering of the track of a typhoon is caused by VRWs with azimuthal wave number one.

In the case of a typhoon-like axisymmetric vortex which has an annulus of high vertical vorticity corresponding to the eyewall (e.g., Kossin and Schubert 2001), the radial gradient of the vertical vorticity at the inside edge of the annulus is opposite in sign to that at the outside edge. There exist cyclonically propagating VRWs at the inside edge, and anticyclonically propagating VRWs at the outside edge. Here "propagating" means "propagating relative to the fluid". The counter-propagation implies the satisfaction of Rayleigh's condition. Further, the cyclonic advection by the axisymmetric vortex is stronger at the outside edge than inside. As a result, the VRWs at the inside and outside edges may be phase-locked with each other, and move cyclonically together. The possibility of phase-lock implies the satisfaction of Fjørtoft's condition. If phase-locked, the counter-propagating VRWs grow by the resonant interaction between them (VRW-VRW interaction). Also in the presence of an annulus of low vertical vorticity in the outer region of an axisymmetric vortex, the growth of phase-locked counter-propagating VRWs is possible.

In the case of a monopole axisymmetric vortex, the radial gradient of the vertical vorticity is everywhere negative. As a result, the VRWs on the vortex propagate anticyclonically everywhere. Because of the absence of the counter-propagating VRWs, disturbances do not grow by the VRW-VRW interaction. However, VRWs in the central region of the vortex generate GWs in the surrounding outer region. It is known that by the interaction between the central VRW and the outer GW (VRW-GW interaction) disturbances grow (e.g., Schecter and Montgomery 2004; Hodyss and Nolan

2008; Zhong et al. 2009; Menelaou et al. 2016).

For example, Schecter and Montgomery (2004) investigated the VRW-GW interaction on a barotropic monopole axisymmetric vortex. By the use of the conservation of wave activity, they obtained an analytical expression of the growth (and damping) rate of the VRW. They showed the following. When the VRW-GW interaction is dominant, the VRW grows. While, when the critical radius damping (Schecter et al. 2002; Schecter and Montgomery 2006) is dominant, the VRW decays. Hodyss and Nolan (2008) examined the VRW-GW interaction on a barocilinic monopole axisymmetric vortex. They showed that the growth due to the VRW-GW interaction is suppressed by the baroclinic structure. Further they examined the case of a vortex having an annulus of high vertical vorticity corresponding to the eyewall, and showed the following. When the annulus is thin, the VRW-VRW interaction is dominant. While, when the annulus is wide, the VRW-GW interaction is dominant. Zhong et al. (2009) showed the existence of growing waves, in addition to VRWs in the central region and GWs in the outer region of an axisymmetric vortex in the shallow water system. In the vicinity of the eyewall, the VRW and GW degenerate into a growing mixed wave. Menelaou et al. (2016) investigated the growth of disturbances on an axisymmetric vortex with nonmonotonic radial distributions of potential vorticity (i.e., satisfying Rayleigh's condition for the VRW-VRW interaction). They showed the following. For the same Rossby number, the smaller Froud number implies the dominance of the VRW-VRW interaction, and the larger implies that of the VRW-GW interaction.

The barotropic (e.g., Heifetz et al. 1999) and baroclinic (e.g., Bretherton 1966) instabilities, which are the typical growing mechanisms of atmospheric disturbances, are caused by the interaction of Rossby waves (RWs), and can be conceptually clearly grasped by the PV-thinking (e.g., Hoskins et al. 1985) in a concise way. The barotropic instability is caused by the horizontal interaction between RWs counter-propagating to each other (i.e., satisfying Rayleigh's condition). If the advection by the environmental flow enables the RWs to be phase-locked (i.e., satisfying Fjørtoft's condition), the resonant interaction between the RWs occur and they grow. The baroclinic instability, which is the mechanism of the growth of midlatitude cyclones, is caused by the vertical interaction between the eastward propagating lower RW and the westward propagating upper RW. The advection by the westerly wind increasing upward enables them to be phase-locked, resulting in the resonant interaction between them and their growth.

However, to our knowledge, there does not yet exist such a clear picture for the VRW-GW interaction as that for the barotropic and baroclinic instability. Of course, the interaction between RWs (or vorticity waves in general) and GWs (i.e., buoyancy waves) has already long been discussed (e.g., Cairns 1979; Sakai 1989), and the VRW-GW interaction here is similar to the well-known Holmboe interaction (see e.g., Carpenter et al. 2011). In particular, as for stratified shear flow instability, Carpenter et al. (2011) discussed in detail the instability in a vertical-zonal 2-dimensional system from the point of wave interaction view. Roughly speaking, the interaction mechanism is described as follows: The vertical circulation induced by the horizontal vorticity perturbation amplifies the buoyancy perturbation, and at the same time the vertical circulation induced by the buoyancy perturbation amplifies the horizontal vorticity perturbation. On one hand, the RW-GW interaction in the vertical-zonal 2-dimensional system occurs between horizontal vorticity and buoyancy waves. On the other hand, the VRW-GW interaction here, which takes place in a 3-dimensional system, occurs between vertical vorticity and buoyancy waves. Different from the RW-GW interaction (including the Holmboe interaction) in the vertical-zonal 2-dimensional system which is accompanied with the vertical circulations induced by the horizontal vorticity and buoyancy perturbations, the VRW-GW interaction here is caused by the horizontal circulation induced by the vertical vorticity perturbation and the vertical circulation induced by the buoyancy perturbation. Although the RW-GW interaction mechanism in the vertical-zonal 2-dimensional system is already conceptually clearly grasped, the VRW-GW interaction mechanism in the 3-dimensional system cannot be grasped as a straightforward extension of the RW-GW interaction mechanism. The propagation and interaction of GWs are conceptually clearly grasped by the buoyancy-vorticity formulation (Harnik et al. 2008), which we call the BV-thinking. In this paper, we propose a simple conceptual model for the VRW-GW interaction base on the BV-thinking.

The organization of this paper is as follows. In section 2, the conceptual model of the VRW-GW interaction is proposed. In section 3, we analytically show the possibility of the VRW-GW interaction in the system linearized about a basic vortex. In section 4, in the linear system, we numerically obtain the growing solution compatible with the conceptual model. In section 5, concluding remarks are given.

2. Conceptual model of VRW-GW interaction

2.1 Basic equations and assumptions

We consider disturbances on a basic axisymmetric vortex. The basic vortex and disturbances are described in a cyclindrical coordinate system (r, θ, z, t), where r is the radius from the center of the basic vortex, θ is the azimuth, z is the height, and t is the time. The fluid is assumed to be confined between two rigid horizontal boundaries at $z = 0$ and $z = H$. Specifically, we assume a stably stratified barotropic Rankine vortex (see

Fig. 1) [Fig. 1]

$$\overline{\zeta} = Z \text{ (positive constant)} \quad \text{for} \quad 0 < r \le R, \quad \text{and} \quad \overline{\zeta} = 0 \quad \text{for} \quad R < r < \infty, \tag{1}$$

where $\overline{\zeta} = \overline{\zeta}(r) = (1/r)d(r\overline{v})/dr$ is the basic vertical vorticity, and $\overline{v} = \overline{v}(r)$ is the basic azimuthal velocity. The basic angular velocity $\overline{\varpi} = \overline{\varpi}(r) = \overline{v}/r$ of the vortex in Eq. (1) is given by

$$\overline{\varpi} = \frac{Z}{2} \quad \text{for} \quad 0 < r \le R, \quad \text{and} \quad \overline{\varpi} = \frac{ZR^2}{2r^2} \quad \text{for} \quad R \le r < \infty. \tag{2}$$

The stable stratification implies that the vertical gradient of the basic buoyancy $\overline{b}$, which is proportional to the basic potential temperature, is positive.

$$\frac{d\overline{b}}{dz} = N^2 > 0,$$

where N is the buoyancy frequency of the basic state, which is assumed to be constant. Because of the piecewise uniform distribution of $\overline{\zeta}$ in Eq. (1), there is a negative radial gradient $d\overline{\zeta}/dr < 0$ of the basic vertical vorticity $\overline{\zeta}$ at $r = R$.

$$\frac{d\overline{\zeta}}{dr} = -Z\delta(r - R), \tag{3}$$

where $\delta(r)$ is Dirac's delta function.

The motion of the fluid is governed by the following equations.

$$
\begin{aligned}
\frac{du}{dt} + \frac{\partial \phi}{\partial r} - \left(f + \frac{v}{r}\right) v = 0, \\
\frac{dv}{dt} + \frac{1}{r}\frac{\partial \phi}{\partial \theta} + \left(f + \frac{v}{r}\right) u = 0, \\
\frac{dw}{dt} + \frac{\partial \phi}{\partial z} - b = 0, \\
\frac{db}{dt} = 0, \\
\frac{1}{r}\frac{\partial}{\partial r}(ru) + \frac{1}{r}\frac{\partial v}{\partial \theta} + \frac{\partial w}{\partial z} = 0,
\end{aligned}
\tag{4}
$$

where $d/dt = \partial/\partial t + u\partial/\partial r + (v/r)\partial/\partial\theta + w\partial/\partial z$, and the Coriolis parameter f is assumed to be constant. The symbols in Eqs. (4) are defined as follows : u, v, and w are respectively the radial, azimuthal, and vertical component of velocity, ϕ is the pressure deviation from a quiescent reference state divided by the reference density, and b, which is called buoyancy, is the potential temperature deviation from the quiescent reference state divided by the reference potential temperature and multiplied by the gravitational acceleration. The first equation of Eqs. (4) is the radial momentum equation. The second is the azimuthal momentum equations. The third is the vertical momentum equation. The fourth is the thermodynamic equation. The fifth is the mass conservation equation with the Boussinesq approximation.

Linearized about the basic vortex in Eq. (1), Eqs. (4) become

$$
\begin{aligned}
\left(\frac{\partial}{\partial t}+\overline{\omega}\frac{\partial}{\partial \theta}\right)u'+\frac{\partial \phi'}{\partial r}-\overline{\xi}v'=0,\\
\left(\frac{\partial}{\partial t}+\overline{\omega}\frac{\partial}{\partial \theta}\right)v'+\frac{1}{r}\frac{\partial \phi'}{\partial \theta}+\overline{\zeta}^a u'=0,\\
\left(\frac{\partial}{\partial t}+\overline{\omega}\frac{\partial}{\partial \theta}\right)w'+\frac{\partial \phi'}{\partial z}-b'=0,\\
\left(\frac{\partial}{\partial t}+\overline{\omega}\frac{\partial}{\partial \theta}\right)b'+N^2w'=0,\\
\frac{1}{r}\frac{\partial}{\partial r}(ru')+\frac{1}{r}\frac{\partial v'}{\partial \theta}+\frac{\partial w'}{\partial z}=0,
\end{aligned}
\tag{5}
$$

where $\overline{\xi}=f+2\overline{\omega}$ is the basic inertial parameter, $\overline{\zeta}^a=f+\overline{\zeta}$ is the basic absolute vertical vorticity, and the primed variables are of the disturbance. Hereafter, the primes are dropped for the presentation simplicity.

From Eqs. (5), the equation of disturbance potential vorticity q is derived.

$$
\left(\frac{\partial}{\partial t}+\overline{\omega}\frac{\partial}{\partial \theta}\right)q+u\frac{d\overline{q}}{dr}=0,
\tag{6}
$$

where $\overline{q}=N^2\overline{\zeta}^a$ is the basic potential vorticity, $q=N^2\zeta+\overline{\zeta}^a\partial b/\partial z$ is the disturbance potential vorticity, $\zeta=(1/r)\partial(rv)/\partial r-(1/r)\partial u/\partial\theta$ is the disturbance vertical vorticity, v is the disturbance azimuthal velocity, u is the disturbance radial velocity, and b is the disturbance buoyancy, which is proportional to the disturbance potential temperature. From the second and third equations of Eqs. (5), the equation of disturbance radial vorticity

η is derived.

$$\left(\frac{\partial}{\partial t} + \overline{\omega}\frac{\partial}{\partial \theta}\right)\eta - \frac{1}{r}\frac{\partial b}{\partial \theta} - f\frac{\partial u}{\partial z} = 0, \tag{7}$$

where $\eta = (1/r)\partial w/\partial\theta - \partial v/\partial z$ is the disturbance radial vorticity, and w is the disturbance vertical velocity.

In order for GWs to exist, the disturbance must have a baroclinic structure. This is because a barotropic structure cannot have vertical circulation. We assume the simplest, that is, the first baroclinic structure of disturbance, having a wavy structure in the azimuthal direction with a wave number m $(\neq 0)$.

$$\begin{aligned} a(r,\theta,z,t) &= \mathrm{Re}\left[\hat{a}(r,t)e^{im\theta}\right]\cos\frac{\pi z}{H} \quad \text{for} \quad a = u, v, \phi, \\ a(r,\theta,z,t) &= \mathrm{Re}\left[\hat{a}(r,t)e^{im\theta}\right]\sin\frac{\pi z}{H} \quad \text{for} \quad a = w, b. \end{aligned} \tag{8}$$

This is of course consistent with the vertical boundary condition, that is, with the existence of free-slip rigid horizontal boundaries on $z = 0$ and $z = H$, and with Eqs. (5). The baroclinic structure in Eqs. (8) implies that the amplitude of ζ is maximum on $z = 0$ and $z = H$, and that the amplitudes of η and b are maximum on $z = H/2$.

2.2 VRW

First, we briefly review the propagation mechanism of VRWs on the basic axisymmetric vortex. When the vertical velocity is neglected, the disturbance buoyancy b vanishes and Eq. (6) of disturbance potential vorticity q is reduced to the equation of disturbance vertical vorticity ζ.

$$\frac{\partial \zeta}{\partial t} = -\overline{\omega}\frac{\partial \zeta}{\partial \theta} - u\frac{d\overline{\zeta}}{dr}. \tag{9}$$

The stretching effect, which is present in the potential vorticity equation (5), is absent in the vorticity equation (9). The negative radial gradient $d\overline{\zeta}/dr < 0$ at $r = R$ in Eq. (3) implies the generation of vertical vorticity perturbation $\zeta > 0$ ($\zeta < 0$) by the radially outward (inward) advection of the basic vertical vorticity $\overline{\zeta}$ across $r = R$. On the assumption of the first baroclinic structure in Eqs. (8), the vertical vorticity perturbation ζ has the maximum amplitude on $z = 0$ and $z = H$. We display ζ on $z = 0$ in a rectangular diagram in which the abscissa is the θ axis pointing to the left, and the ordinate is the r axis pointing upwards (see Fig. 2). Fig. 2

We assume a wavy disturbance with $\zeta > 0$ and $\zeta < 0$ (see the top part of Fig. 2). In Fig. 2, the black curves are the Iso-($\overline{\zeta}+\zeta$) lines. The disturbance is advected downstream (that is, cyclonically) by the basic vortex flow. This is expressed by the first term $-\overline{\omega}\partial\zeta/\partial\theta$ on the RHS of Eq. (9). In addition to the cyclonic advection, the disturbance azimuthally propagates. The reason is as follows. Around $\zeta > 0$ and $\zeta < 0$, there are induced cyclonic and anticyclonic horizontal circulations, respectively. The associated radial velocity perturbation u (black arrows ↑↓↑ in the top part of Fig. 2) advects the basic vertical vorticity $\overline{\zeta}$. This is expressed by the second term $-ud\overline{\zeta}/dr$

on the RHS of Eq. (9). The radial advection of $\overline{\zeta}$ generates new $\zeta > 0$ and $\zeta < 0$ on the upstream side of the old $\zeta > 0$ and $\zeta < 0$, respectively (see the bottom part of Fig. 2). As a result, the disturbance propagates upstream (that is, anticyclonically) at $r = R$. The disturbance on $z = H$ also propagates upstream. This is the VRW. Because of the dominance of cyclonic advection by the basic angular velocity $\overline{\omega} > 0$ over the anticyclonic propagation due to the negative radial gradient $d\overline{\zeta}/dr < 0$, the VRW moves cyclonically at $r = R$.

2.3 GW

Second, we briefly review the propagation mechanism of GWs. The stable stratification $N^2 = d\overline{b}/dz > 0$ implies the generation of buoyancy perturbation $b > 0$ ($b < 0$) by the downward (upward) advection of the basic buoyancy $\overline{b}$. Because of this, there may exist several kinds of GWs. Here we consider a GW which is generated by the cyclonically moving VRW at $r = R$, and is cyclonically propagating at some outer radius $r = \tilde{R}$ ($> R$). When the radial velocity u is neglected, the motion becomes (θ, z) two dimensional, and Eq. (7) of disturbance radial vorticity η is reduced to the two dimensional form. This is given together with the fourth equation of

Eqs. (5) by

$$\frac{\partial \eta}{\partial t} = -\overline{\omega}\frac{\partial \eta}{\partial \theta} + \frac{1}{r}\frac{\partial b}{\partial \theta}, \tag{10}$$
$$\frac{\partial b}{\partial t} = -\overline{\omega}\frac{\partial b}{\partial \theta} - w\frac{d\overline{b}}{dz}. \tag{11}$$

Because of the first baroclinic structure in Eqs. (8), the η and b perturbations vanish on $z = 0$ and $z = H$, and their amplitude is maximum on $z = H/2$. We display $\{\eta, b\}$ in a rectangular diagram, in which the abscissa is the θ axis pointing to the left, and the ordinate is the z axis pointing upwards (see Fig. 3). Fig. 3

We assume a wavy disturbance with $\{\eta > 0,\ b < 0\}$ and $\{\eta < 0,\ b > 0\}$ on $z = H/2$ (see the top part of Fig. 3). In Fig. 3, the black curves are the Iso-$(\overline{b}+b)$ lines, and red circles with arrows represent η. The disturbance is advected downstream (that is, cyclonically) by the basic vortex flow. This is expressed by the first terms $-\overline{\omega}\partial\eta/\partial\theta$ and $-\overline{\omega}\partial b/\partial\theta$ on the RHSs of Eqs. (10) and (11). In addition to the cyclonic advection, the disturbance azimuthally propagates. The reason is as follows. Around the positive and negative radial vorticity perturbations $\eta > 0$ and $\eta < 0$, there are induced clockwise and anticlockwise vertical circulations, respectively. The associated vertical velocity perturbation w (red arrows ↓↑↓ in the middle part of Fig.3) advects the basic buoyancy $\overline{b}$. This is expressed by the second term $-wd\overline{b}/dz$ of the RHS of Eq. (11). The vertical advection of $\overline{b}$ generates new $b < 0$ and $b > 0$ downstream side of the old $\eta > 0$ and $\eta < 0$, that is, of the old $b < 0$ and $b > 0$, respectively (compare the middle part with the top part of Fig. 3).

At the same time, the positive and negative buoyancy perturbations $b > 0$ and $b < 0$ imply the horizontal gradient of buoyancy force (black arrows ↑↓ in the bottom part of Fig. 3). The gradient generates η. This is expressed by the second term $(1/r)\partial b/\partial\theta$ on the RHS of Eq. (10). The buoyancy gradient generates new $\eta > 0$ and $\eta < 0$ downstream side of the old $b < 0$ and $b > 0$, that is, of the old $\eta > 0$ and $\eta < 0$, respectively (compare the bottom part with the top part of Fig. 3).

As a result, the wavy disturbance with $\{\eta > 0,\ b < 0\}$ and $\{\eta < 0,\ b > 0\}$ propagates downstream (that is, cyclonically) on $z = H/2$. This is the GW. Since both the advection and propagation are downstream (that is, cyclonic), the GW moves cyclonically on $z = H/2$.

The cyclonically propagating GW resonantly interacts with the anti-cyclonically propagating VRW as depicted in Subsection 2.4. There exists another GW with b and η in phase which propagates anti-cyclonically with respect to the basic flow and does not directly resonantly interact with the anti-cyclonically propagating VRW. However, the anti-cyclonically propagating GW may indirectly contribute to the resonant VRW-GW interaction as in the case of the resonant interaction between GWs (Rabinovich et al.

2011).

2.4 VRW-GW interaction

We assume weak vertical motion in the central region near $r = R$ and weak radial motion in the outer region near $r = \tilde{R}$ so that the above mentioned VRW at $r = R$ and GW at $r = \tilde{R}$ can basically exist. Because of the first baroclinic structure in Eqs. (8), the amplitude of the VRW is maximum on $z = 0$ and $z = H$. The vertical vorticity perturbation ζ of the lower VRW is opposite-signed to that of the upper VRW. While, the amplitude of the GW is maximum on $z = H/2$. Since the VRW anticyclonically propagates and the GW cyclonically propagates, they are counter-propagating to each other. Further, since both the VRW and GW move cyclonically, they may satisfy Fjørtoft's condition for instability, and they may be phase-locked with each other. Here we assume that the counter-propagating VRW and GW are phase-locked with phase difference $\pi/2$. Comoving with the phase-locked VRW and GW, we display the disturbance in a rectangular diagram consisting of three parts in Fig. 4. The corresponding 3-dimensional and plan views are depicted in Fig. 5, and Fig. 6, respectively. Fig. 4

In the top, middle, and bottom parts of Fig. 4, the abscissa is the θ axis Fig. 5
pointing to the left. In the top part, the vertical vorticity perturbation ζ of Fig. 6
the upper VRW at $r = R$ is depicted. The ordinate is the r axis pointing

downwards. The black curve is the Iso-$(\bar{\zeta}+\zeta)$ line.

In the middle part, the radial vorticity perturbation η and buoyancy perturbation b of the GW at $r=\tilde{R}$ are depicted. The ordinate is the z axis pointing upwards. The black curve is the Iso-$(\bar{b}+b)$ line, and the red circles with arrows represent η.

In the bottom part, the vertical vorticity perturbation ζ of the lower VRW at $r=R$ is depicted. The ordinate is the r axis pointing upwards. The black curve is the Iso-$(\bar{\zeta}+\zeta)$ line.

The upper and lower ζ of VRWs at $r=R$ induce radial velocities $u>0$ and $u<0$ (black arrows $\uparrow\downarrow\uparrow$ in the top and bottom parts of Fig. 4). The radial velocities $u>0$ and $u<0$ generate vertical divergence (VD) and convergence (VC) (black circles with VD and with VC) at $r=\tilde{R}$, respectively. The upper VC and lower VD cause upward velocity $w>0$ (black short uparrow $\Uparrow$ in the middle part of Fig. 4), which increases the amplitude of $b<0$. In the same way, the upper VD and lower VC cause downward velocity $w<0$ (black short downarrow $\Downarrow$ in the middle of Fig. 4), which increases the amplitude of $b>0$.

At the same time, the vertical velocities $w>0$ and $w<0$ (red arrows $\downarrow\uparrow\downarrow$ in the middle part of Fig. 4) around the middle η generate horizontal divergence (HD) and convergence (HC) on the upper and lower levels at $r=\tilde{R}$ (red circles with HD and with HC). The upper HD and HC cause inward and outward velocities $u < 0$ and $u > 0$ on $z = H$ (red short uparrow $\Uparrow$ and downarrow $\Downarrow$ in the top part of Fig. 4), which increase the amplitude of the upper $\zeta < 0$ and $\zeta > 0$, respectively. In the same way, the lower HD and HC cause inward and outward velocities $u < 0$ and $u > 0$ on $z = 0$ (red short downarrow $\Downarrow$ and uparrow $\Uparrow$ in the bottom part of Fig. 4), which increase the amplitude of the lower $\zeta < 0$ and $\zeta > 0$, respectively.

As a result, the VRW and GW mutually reinforce and grow.

3. Analytical consideration

In this section, the possibility of the resonant VRW-GW interaction is analytically shown. Most of the equations of this section (and their deformation) in themselves are not important or essential. They are presented only for the purpose of deriving Equation (36) which shows the possibility of the resonant interaction between the central VRW and the outer GW.

3.1 Nondimensional hydrostatic system

For the mathematical simplicity, here and hereafter we assume the hydrostatic balance, which means the replacement of the third equation of Eqs. (5) with the hydrostatic equation $\partial\phi/\partial z = b$. Then, the last three equations of Eqs. (5) are combined into one equation,

$$\left(\frac{\partial}{\partial t}+\overline{\varpi}\frac{\partial}{\partial \theta}\right)\frac{\partial^2 \phi}{\partial z^2}-N^2\left\{\frac{1}{r}\frac{\partial}{\partial r}(ru)+\frac{1}{r}\frac{\partial v}{\partial \theta}\right\}=0. \tag{12}$$

In the mode assumed in Eqs. (8), the first two equations of Eqs. (5) and (12) become

$$\begin{aligned}
\left(\frac{\partial}{\partial t}+im\overline{\varpi}\right)\hat{u}+\frac{\partial \hat{\phi}}{\partial r}-\overline{\xi}\hat{v}=0,\\
\left(\frac{\partial}{\partial t}+im\overline{\varpi}\right)\hat{v}+\frac{im}{r}\hat{\phi}+\overline{\zeta}^a\hat{u}=0,\\
\left(\frac{\partial}{\partial t}+im\overline{\varpi}\right)\hat{\phi}+\frac{N^2H^2}{\pi^2}\left\{\frac{1}{r}\frac{\partial}{\partial r}(r\hat{u})+\frac{im}{r}\hat{v}\right\}=0.
\end{aligned} \tag{13}$$

We introduce the following nondimensional variables,

$$t\to\frac{1}{Z}t,\quad r\to Rr,\quad (\overline{\varpi},\overline{\xi},\overline{\zeta}^a)\to Z(\overline{\varpi},\overline{\xi},\overline{\zeta}^a)\quad (\hat{u},\hat{v})\to[\hat{u}](\hat{u},\hat{v}),\quad \hat{\phi}\to[\hat{\phi}]\hat{\phi}, \tag{14}$$

where Z and R are respectively the central vorticity and radius of the basic Rankine vortex in Eq. (1), and $[\hat{u}]$ and $[\hat{\phi}]$ are respectively the representative absolute values of $\hat{u}$ and $\hat{\phi}$. From the balance in the first two equations of Eqs. (13), the representative values $[\hat{u}]$ and $[\hat{\phi}]$ are related as

$$[\hat{\phi}]=RZ[\hat{u}]. \tag{15}$$

By the substitution of Eqs. (14) and (15), Eqs. (13) are nondimensionalized as follows,

$$\begin{aligned} \left(\frac{\partial}{\partial t} + im\overline{\omega}\right)\hat{u} + \frac{\partial\hat{\phi}}{\partial r} - \overline{\xi}\hat{v} = 0, \\ \left(\frac{\partial}{\partial t} + im\overline{\omega}\right)\hat{v} + \frac{im}{r}\hat{\phi} + \overline{\zeta}^a\hat{u} = 0, \\ \left(\frac{\partial}{\partial t} + im\overline{\omega}\right)\hat{\phi} + \gamma\left\{\frac{1}{r}\frac{\partial}{\partial r}(r\hat{u}) + \frac{im}{r}\hat{v}\right\} = 0 \quad \text{with} \quad \gamma = \left(\frac{NH}{\pi RZ}\right)^2, \end{aligned} \tag{16}$$

where the nondimensional basic variables $\overline{\omega}$, $\overline{\xi}$, and $\overline{\zeta}^a$ are respectively given by

$$\begin{aligned} \overline{\omega} = \frac{1}{2} \quad \text{for} \quad 0 < r < 1, \quad \text{and} \quad \overline{\omega} = \frac{1}{2r^2} \quad \text{for} \quad 1 < r < \infty, \\ \overline{\xi} = 1 + \frac{f}{Z} \quad \text{for} \quad 0 < r < 1, \quad \text{and} \quad \overline{\xi} = \frac{1}{r^2} + \frac{f}{Z} \quad \text{for} \quad 1 < r < \infty, \\ \overline{\zeta}^a = 1 + \frac{f}{Z} \quad \text{for} \quad 0 < r < 1, \quad \text{and} \quad \overline{\zeta}^a = \frac{f}{Z} \quad \text{for} \quad 1 < r < \infty. \end{aligned} \tag{17}$$

For a fixed wave number m, the nondimensional equations in Eqs. (16) includes two parameters f/Z and γ. We assume a typical tropical cyclone at latitude $\approx 20°$ with the central vorticity $Z \approx$ a few $\times 10^{-3}$ s^{-1}. Then, because of $f \approx 5 \times 10^{-5}$ s^{-1}, the first parameter is estimated as $f/Z \approx [5 \times 10^{-5}]/[\text{a few } \times 10^{-3}]$. So, we set

$$\frac{f}{Z} = 0.02$$

for the numerical calculation in section 4. We assume the Rankine radius $R \approx 5 \times 10^4$ m (representative radius of maximum wind) and the fluid depth

$H \approx 10^4$ m (representative depth of the troposphere). The representative value of the buoyancy frequency is $N \approx 10^{-2}$ s^{-1}. However, because of the vertical convection together with diabatic heating/cooling in the central typhoon region and therearoud, the buyoyancy frequency is reduced there. So, we assume $0 < N \lesssim 5 \times 10^{-3}$ s^{-1}. Then, the second parameter is estimated as

$$0 < \gamma = \left(\frac{NH}{\pi RZ}\right)^2 \lesssim \left(\frac{5 \times 10^{-3} \times 10^4}{\pi \times 5 \times 10^4 \times [\text{a few} \times 10^{-3}]}\right)^2 = \left(\frac{1}{\text{a few } \times \pi}\right)^2 \approx 0.02.$$

3.2 Vorticity and divergence system

From the first two equations of Eqs. (16), the following vertical vorticity and horizontal divergence equations are derived,

$$\left(\frac{\partial}{\partial t} + im\overline{\omega}\right)\hat{\zeta} + \frac{d\overline{\zeta}^a}{dr}\hat{u} + \overline{\zeta}^a \hat{D} = 0,$$
$$\left(\frac{\partial}{\partial t} + im\overline{\omega}\right)\hat{D} + \hat{\partial}^2\hat{\phi} + 2\frac{d\overline{\omega}}{dr}(im\hat{u} - \hat{v}) - \overline{\xi}\hat{\zeta} = 0, \quad (18)$$

where $\hat{\zeta} = (1/r)(\partial/\partial r)(r\hat{v}) - (im/r)\hat{u}$ is the disturbance vertical vorticity, $\hat{D} = (1/r)(\partial/\partial r)(r\hat{u}) + (im/r)\hat{v}$ is the disturbance horizontal divergence, and $\hat{\partial}^2 = (1/r)(\partial/\partial r)r(\partial/\partial r) - (m^2/r^2)$ is the horizontal Laplacian operator. The disturbance horizontal velocity $(\hat{u}, \hat{v})$, which is assumed to vanish at infinity, can be decomposed into the rotational component (u^R, v^R) and divergent component (u^D, v^D), which are respectively written in terms of the stream function Ψ and the velocity potential Φ as

$$\hat{u} = u^R + u^D = -\frac{im}{r}\Psi + \frac{\partial \Phi}{\partial r}, \quad \hat{v} = v^R + v^D = \frac{\partial \Psi}{\partial r} + \frac{im}{r}\Phi. \tag{19}$$

The disturbance vertical vorticity $\hat{\zeta}$ and horizontal divergence $\hat{D}$ are respectively expressed in terms of the stream function Ψ and the velocity potential Φ as

$$\hat{\zeta} = \hat{\partial}^2 \Psi \quad \text{and} \quad \hat{D} = \hat{\partial}^2 \Phi. \tag{20}$$

By the inversion of Eqs. (20), the stream function Ψ and the velocity potential Φ are respectively expressed in terms of the Green function $G(r, r')$ as functionals of $\hat{\zeta}$ and $\hat{D}$,

$$\Psi(r,t) = \int_0^\infty dr' G(r,r')\hat{\zeta}(r',t) \quad \text{and} \quad \Phi(r,t) = \int_0^\infty dr' G(r,r')\hat{D}(r',t), \tag{21}$$

where the Green function is the solution of

$$\hat{\partial}^2 G(r,r') = \delta(r-r') \ \text{ under boundary conditions } \ \lim_{r\to 0} G(r,r') < \infty \ \text{ and } \ \lim_{r\to\infty} G(r,r') = 0,$$

and is given by

$$G(r,r') = -\frac{r'}{2m}\left(\frac{r}{r'}\right)^m \ \text{ for } \ r < r', \ \text{ and } \ G(r,r') = -\frac{r'}{2m}\left(\frac{r'}{r}\right)^m \ \text{ for } \ r > r'. \tag{22}$$

Substituting Eqs. (19) and (21) into Eqs. (18), together with the third equation of Eqs. (16), gives a closed system for $\hat{\zeta}$, $\hat{D}$, and $\hat{\phi}$,

$$\left(\frac{\partial}{\partial t} + im\overline{\omega}\right)\hat{\zeta}(r,t) - \frac{im}{r}\frac{d\overline{\zeta}^a}{dr}\int_0^\infty dr' G(r,r')\hat{\zeta}(r',t) + \frac{d\overline{\zeta}^a}{dr}\frac{\partial}{\partial r}\int_0^\infty dr' G(r,r')\hat{D}(r',t) + \overline{\zeta}^a\hat{D}(r,t) = 0, \quad (23)$$

$$\left(\frac{\partial}{\partial t} + im\overline{\omega}\right)\hat{D}(r,t) + \hat{\partial}^2\hat{\phi}(r,t) + i2m\frac{d\overline{\omega}}{dr}\left(\frac{\partial}{\partial r} - \frac{1}{r}\right)\int_0^\infty dr' G(r,r')\hat{D}(r',t) + 2\frac{d\overline{\omega}}{dr}\left(\frac{m^2}{r} - \frac{\partial}{\partial r}\right)\int_0^\infty dr' G(r,r')\hat{\zeta}(r',t) - \overline{\xi}\hat{\zeta}(r,t) = 0, \quad (24)$$

$$\left(\frac{\partial}{\partial t} + im\overline{\omega}\right)\hat{\phi}(r,t) + \gamma\hat{D}(r,t) = 0. \quad (25)$$

3.3 Equation of VRW

Eliminating the horizontal divergence $\hat{D}$ from the first equation of Eqs. (18) and Eq. (25) gives the potential vorticity equation.

$$\left(\frac{\partial}{\partial t} + im\overline{\omega}\right)\hat{q} + \frac{d\overline{q}}{dr}\hat{u} = 0, \quad (26)$$

where $\overline{q} = \gamma\overline{\zeta}^a$ is the basic potential vorticity, and $\hat{q} = \gamma\hat{\zeta} - \overline{\zeta}^a\hat{\phi}$ is the disturbance potential vorticity. For the assumed Rankine vortex in Eqs. (1), the basic absolute vertical vorticity $\overline{\zeta}^a = \overline{\zeta} + f/Z$ is piecewise uniform and has a singular radial gradient in Eq. (3), and so the basic potential vorticity $\overline{q} = \gamma\overline{\zeta}^a$ has the same singularity,

$$\frac{d\overline{\zeta}^a}{dr} = -\delta(r-1) \quad \text{and} \quad \frac{d\overline{q}}{dr} = -\gamma\delta(r-1). \quad (27)$$

From Eqs. (26) and (27), the potential vorticity perturbation $\hat{q}(r,t)$ consists of a singular part $\hat{q}_R(t)\delta(r-1)$ and a nonsingular part $\tilde{q}(r,t)$,

$$\hat{q}(r,t) = \hat{q}_R(t)\delta(r-1) + \tilde{q}(r,t).$$

The singular part comes from the singular part $\hat{\zeta}_R(t)\delta(r-1)$ of the vertical vorticity perturbation,

$$\hat{\zeta}(r,t) = \hat{\zeta}_R(t)\delta(r-1) + \tilde{\zeta}(r,t), \tag{28}$$

which is caused by the piecewise uniform distribution of the basic vertical vorticity $\overline{\zeta}$ in Eqs. (1). From Eq. (26), the nonsingular part $\tilde{q} = \gamma\tilde{\zeta} - \overline{\zeta}^a\hat{\phi}$ satisfies

$$\left(\frac{\partial}{\partial t} + im\overline{\omega}\right)\tilde{q} = 0.$$

Under a null initial condition $\tilde{q}(r,0) = 0$, this equation implies that $\tilde{q}(r,t) = 0$. The null initial condition is naturally assumed since a perturbation $\hat{q} \neq 0$ is not generated by the displacement of fluid particles in the region of uniform $\overline{q}$. In other words, the non-zero perturbation $\hat{q}$ can be generated only by fluid particles crossing $r = 1$, resulting in the singular perturbation. The vanishing $\tilde{q}(r,t) = 0$ implies that

$$\tilde{\zeta}(r,t) = \frac{1}{\gamma}\overline{\zeta}^a\hat{\phi}(r,t). \tag{29}$$

Substituting Eq. (28) into Eq. (23), and calculating $\lim_{\epsilon\to 0}\int_{1-\epsilon}^{1+\epsilon} dr\ (\cdots)$ gives

$$\left\{\frac{\partial}{\partial t} + im\overline{\omega}(1)\right\}\hat{\zeta}_R(t) + imG(1,1)\hat{\zeta}_R(t) + im\int_0^\infty dr'\ G(1,r')\tilde{\zeta}(r',t) - \int_0^\infty dr'\ \left[\frac{\partial G(r,r')}{\partial r}\right]_{r=1}\hat{D}(r',t) = 0. \tag{30}$$

Further substituting Eqs. (22) and (29) into Eq. (30) gives

$$\frac{\partial}{\partial t}\hat{\zeta}_R(t) + \frac{im}{2}\hat{\zeta}_R(t) - \frac{i}{2}\hat{\zeta}_R(t) = \frac{i}{2\gamma}\left(1+\frac{f}{Z}\right)\int_0^1 dr\ r^{1+m}\hat{\phi}(r,t) + \frac{1}{2}\int_0^1 dr\ r^{1+m}\hat{D}(r,t) + \frac{i}{2\gamma}\frac{f}{Z}\int_1^\infty dr\ r^{1-m}\hat{\phi}(r,t) - \frac{1}{2}\int_1^\infty dr\ r^{1-m}\hat{D}(r,t), \tag{31}$$

where $\overline{\omega}(1) = 1/2$, $\overline{\zeta}^a = 1 + f/Z$ for $0 < r < 1$, and $\overline{\zeta}^a = f/Z$ for $1 < r < \infty$ were used. This is the equation of the VRW on $r = 1$. The second term on the LHS of Eq. (31) represents the cyclonic advection by the basic angular velocity $\overline{\omega}(1) = 1/2$. The third term represents the anticyclonic propagation due to the basic vertical vorticity gradient $d\overline{\zeta}^a/dr = -\delta(r-1)$. The terms on the RHS of Eq. (31) represent the interaction between the VRW on $r = 1$ and the GW in the inner $0 < r < 1$ and outer $1 < r < \infty$ regions.

3.4 Equation of GW

Apart from the singular part, which leads to Eq. (31), Eq. (23) becomes identical to Eq. (25) because of Eq. (29). As for the singular part of Eq. (24), substituting Eq. (28) into Eq. (24), and calculating $\lim_{\epsilon\to 0}\int_{1-\epsilon}^{1+\epsilon} dr\,(\cdots)$ gives

$$\lim_{\epsilon\to 0}\left[\frac{\partial\hat{\phi}(r,t)}{\partial r}\right]_{1-\epsilon}^{1+\epsilon} = \overline{\xi}(1)\hat{\zeta}_R(t) = \left(1+\frac{f}{Z}\right)\hat{\zeta}_R(t). \tag{32}$$

So, the first radial derivative of $\hat{\phi}(r,t)$ is discontinuous at $r=1$. Substituting Eqs. (28) and (29) into Eq. (24), together with Eq. (25), for $r\neq 1$ gives

$$\begin{aligned}
&\left(\frac{\partial}{\partial t}+im\overline{\omega}\right)\hat{D}(r,t)+\hat{\partial}^2\hat{\phi}(r,t)+i2m\frac{d\overline{\omega}}{dr}\left(\frac{\partial}{\partial r}-\frac{1}{r}\right)\int_0^\infty dr' G(r,r')\hat{D}(r',t)\\
&\qquad\qquad +2\frac{d\overline{\omega}}{dr}\left(\frac{m^2}{r}-\frac{\partial}{\partial r}\right)G(r,1)\hat{\zeta}_R(t)\\
&\qquad\qquad +\frac{2}{\gamma}\frac{d\overline{\omega}}{dr}\left(\frac{m^2}{r}-\frac{\partial}{\partial r}\right)\int_0^\infty dr' G(r,r')\overline{\zeta}^a(r')\hat{\phi}(r',t)-\frac{\overline{\zeta}^a\overline{\xi}}{\gamma}\hat{\phi}(r,t)=0,\\
&\left(\frac{\partial}{\partial t}+im\overline{\omega}\right)\hat{\phi}(r,t)+\gamma\hat{D}(r,t)=0 \qquad \text{for} \quad r\neq 1.
\end{aligned} \tag{33}$$

Further substituting Eqs. (22) into Eqs. (33) gives

$$\begin{aligned}
&\frac{\partial}{\partial t}\begin{bmatrix}\hat{D}(r,t)\\ \hat{\phi}(r,t)\end{bmatrix}+\begin{bmatrix} im\overline{\omega} & 0\\ 0 & im\overline{\omega}\end{bmatrix}\begin{bmatrix}\hat{D}(r,t)\\ \hat{\phi}(r,t)\end{bmatrix}+\begin{bmatrix} 0 & \hat{\partial}^2-\dfrac{\overline{\zeta}^a\overline{\xi}}{\gamma}\\ \gamma & 0\end{bmatrix}\begin{bmatrix}\hat{D}(r,t)\\ \hat{\phi}(r,t)\end{bmatrix}\\
&+\begin{bmatrix} i2m\dfrac{d\overline{\omega}}{dr}\left(\dfrac{\partial}{\partial r}-\dfrac{1}{r}\right)\displaystyle\int_0^\infty dr' G(r,r') & \dfrac{2}{\gamma}\dfrac{d\overline{\omega}}{dr}\left(\dfrac{m^2}{r}-\dfrac{\partial}{\partial r}\right)\displaystyle\int_0^\infty dr' G(r,r')\overline{\zeta}^a(r')\\ 0 & 0\end{bmatrix}\begin{bmatrix}\hat{D}(r',t)\\ \hat{\phi}(r',t)\end{bmatrix}\\
&=\begin{bmatrix}(m+1)\dfrac{d\overline{\omega}}{dr}r^{-(m+1)}\hat{\zeta}_R(t)\\ 0\end{bmatrix} \qquad \text{for} \quad r\neq 1.
\end{aligned} \tag{34}$$

This is the equation of the GW. The second term on the LHS of Eq. (34) represents the cyclonic advection by the basic angular velocity $\overline{\omega}(r)$. The third term represents the azimuthal (and radial) propagation due to the stable stratification $\gamma > 0$, and the inertial oscillation due to $\overline{\zeta}^a\overline{\xi} > 0$. The fourth term represents the effect of $d\overline{\omega}/dr \neq 0$. The term on the RHS of Eq. (34) represents the interaction between the GW and the VRW on $r = 1$. Since $d\overline{\omega}/dr = 0$ in the inner region $0 < r < 1$, the terms including $d\overline{\omega}/dr$ vanish there. In particular, the interaction term exists only in the outer region $1 < r < \infty$.

3.5 Interaction between VRW and GW

Since the RHS of Eq. (34), which represents the interaction between the VRW and GW, exists only in the outer region, the mutual interaction is expected to take place between the VRW on $r = 1$ and the GW in the outer region $1 < r < \infty$. From Eqs. (31) and (34), the primary interaction between the VRW on $r = 1$ and the GW in the outer region $1 < r < \infty$ is described by the following equation,

$$\frac{\partial}{\partial t}\hat{\zeta}_R(t) + \cdots = -\frac{1}{2}\int_1^\infty dr\ r^{1-m}\hat{D}(r,t),$$
$$\frac{\partial}{\partial t}\hat{D}(r,t) + \cdots = -(m+1)\left|\frac{d\overline{\omega}(r)}{dr}\right| r^{-(m+1)}\hat{\zeta}_R(t). \qquad (35)$$

Differentiating the first equation of Eqs. (35) with respect to time t, and then substituting the second equation gives

$$\frac{\partial^2}{\partial t^2}\hat{\zeta}_R(t)+\cdots=\sigma^2\hat{\zeta}_R(t) \quad \text{with} \quad \sigma^2=\frac{m+1}{2}\int_1^\infty dr\, r^{-2m}\left|\frac{d\overline{\omega}(r)}{dr}\right|=\left(\frac{1}{2}\right)^2, \tag{36}$$

where $d\overline{\omega}/dr=-1/r^3$ was used. Since the constant $\sigma^2=(1/2)^2$ in Eq. (36) is positive, we can expect exponential growth of $\hat{\zeta}_R(t)\sim e^{\sigma t}=e^{(1/2)t}$ by the interaction.

The minus signs of the RHSs of Eqs. (35) imply the following. If $\hat{\zeta}_R(t)$ on $r=1$ and $\hat{D}(r,t)$ at some radius $\tilde{r}>1$ are phase-locked with a phase difference π, then they amplify each other, and then they may exponentially grow.

The amplifying mechanism described by the first equation of Eqs. (35) is simple. The horizontal convergence $\hat{D}(r,t)<0$ at the radius $\tilde{r}>1$ (HC in Fig. 4) is accompanied with a radially outflow at $r=1$ (⇓ in the top of Fig. 4, and ⇑ in the bottom of Fig. 4), which advects the basic vertical vorticity outward and amplifies the phase-locked positive vertical vorticity perturbation $\hat{\zeta}_R(t)>0$ at $r=1$ ($\zeta>0$ in Fig. 4). In the same way, the horizontal divergence $\hat{D}(r,t)>0$ at the radius $\tilde{r}>1$ (HD in Fig. 4) is accompanied with a radially inflow at $r=1$ (⇑ in the top of Fig. 4, and ⇓ in the bottom of Fig. 4), which advects the basic vertical vorticity inward and amplifies the phase-locked negative vertical vorticity perturbation $\hat{\zeta}_R(t)<0$

at $r = 1$ ($\zeta < 0$ in Fig. 4).

While, the amplifying mechanism described by the second equation of Eqs. (35) is somewhat complicated. Let us consider the lowermost level on $z = 0$. The positive vertical vorticity perturbation $\hat{\zeta}_R(t) > 0$ at $r = 1$ on $z = 0$ ($\zeta > 0$ in the bottom of Fig. 4) is accompanied with a cyclonic horizontal circulation (↓↑ in the bottom of Fig. 4). The radially outflow branch of the circulation (the rightmost ↑ in the bottom of Fig. 4), which lies one quarter wavelength upstream, may cause updraft at the radius $\tilde{r} > 1$ (⇑ in the middle of Fig. 4). The updraft amplifies the negative buoyancy perturbation (i.e., negative potential temperature perturbation) ($b < 0$ in the middle of Fig.4) of the phase-locked gravity wave which is anticyclonically propagating. The anticyclonically propagating negative buoyancy perturbation is accompanied with a vertical circulation (↑↓ in the middle of Fig. 4). The updraft branch of the circulation (↑ in the middle of Fig. 4), which lies one quarter wavelength downstream, amplifies the phase-locked horizontal convergence $\hat{D}(r, t) < 0$ at the radius $\tilde{r} > 1$ on $z = 0$ (HC in the bottom of Fig. 4). In the same way, the negative vertical vorticity perturbation $\hat{\zeta}_R(t) < 0$ at $r = 1$ on $z = 0$ ($\zeta < 0$ in the bottom of Fig. 4) is accompanied with an anticyclonic horizontal circulation (↑↓ in the bottom of Fig.4). The radially inflow branch of the circulation (↓ in the bottom of Fig. 4), which lies one quarter wavelength upstream, may cause downdraft at the radius $\tilde{r} > 1$ ($\Downarrow$ in the middle of Fig. 4). The downdraft amplifies the positive buoyancy perturbation (i.e., positive potential temperature perturbation) ($b > 0$ in the middle of Fig. 4) of the phase-locked gravity wave which is anticyclonically propagating. The anticyclonically propagating positive buoyancy perturbation is accompanied with a vertical circulation ($\downarrow\uparrow$ in the middle of Fig. 4). The downdraft branch of the circulation, which lies one quarter wavelength downstream, amplifies the phase-locked horizontal divergence $\hat{D}(r,t) > 0$ at the radius $\tilde{r} > 1$ on $z = 0$ (HD in the bottom of Fig. 4). Also on the uppermost level $z = H$, the similar reasoning is applied.

4. Numerical calculation

In this section, we numerically obtain a growing solution whose spatial pattern is compatible with the conceptual model of the resonant VRW-GW interaction proposed in Section 2. Although this section includes many equations and their deformation and rearrangement, they themselves are not important or essential. They are presented only for the purpose of displaying figures in Fig. 7 which confirm the validity of the proposed conceptual model.

For the assumed Rankine-vortex in Eqs. (1), the vorticity perturbation whose radial dependence is expressed in terms of Dirac's delta function is generated by the singular radial gradient of the basic vorticity in Eq. (3). The singular dependence cannot be numerically represented. So, in order to numerically obtain the solution of the nondimensional linearized equations (16), we replace the discontinuous basic Rankine vortex in Eqs. (1) by the following continuous Rankine-like vortex,

$$\begin{aligned}
&\overline{\zeta} = Z \quad \text{for} \quad 0 < r < R - \varepsilon, \\
&\overline{\zeta} = \frac{Z(R+\varepsilon)}{2\varepsilon} - \frac{Z}{2\varepsilon} r \quad \text{for} \quad R - \varepsilon < r < R + \varepsilon, \\
&\overline{\zeta} = 0 \quad \text{for} \quad R + \varepsilon < r < \infty,
\end{aligned} \tag{37}$$

where we assume $\varepsilon/R \approx 1/10$. Instead of Eqs. (2), the basic angular velocity $\overline{\omega} = \overline{\omega}(r)$ is given by

$$\begin{aligned}
&\overline{\omega} = \frac{Z}{2} \quad \text{for} \quad 0 < r < R - \varepsilon, \\
&\overline{\omega} = -\frac{Z}{6\varepsilon} r + \frac{Z(R+\varepsilon)}{4\varepsilon} - \frac{Z(R-\varepsilon)^3}{12\varepsilon} \frac{1}{r^2} \quad \text{for} \quad R - \varepsilon < r < R + \varepsilon, \\
&\overline{\omega} = \frac{Z(3R^2 + \varepsilon^2)}{6} \frac{1}{r^2} \quad \text{for} \quad R + \varepsilon < r < \infty.
\end{aligned}$$

The nondimensional linearized equations (16) are unchanged except that the nondimensional basic variables $\overline{\omega}$, $\overline{\xi}$, and $\overline{\zeta}^a$ in Eqs. (17) are respectively replaced by

$$\begin{aligned}
&\overline{\omega} = \frac{1}{2} \quad \text{for} \quad 0 < r < 1 - \tilde{\varepsilon}, \\
&\overline{\omega} = -\frac{1}{6\tilde{\varepsilon}} r + \frac{1+\tilde{\varepsilon}}{4\tilde{\varepsilon}} - \frac{(1-\tilde{\varepsilon})^3}{12\tilde{\varepsilon}} \frac{1}{r^2} \quad \text{for} \quad 1 - \tilde{\varepsilon} < r < 1 + \tilde{\varepsilon}, \\
&\overline{\omega} = \frac{3 + \tilde{\varepsilon}^2}{6} \frac{1}{r^2} \quad \text{for} \quad 1 + \tilde{\varepsilon} < r < \infty,
\end{aligned}$$

$$
\begin{aligned}
\overline{\xi} &= 1 + \frac{f}{Z} \quad \text{for} \quad 0 < r < 1 - \tilde{\varepsilon}, \\
\overline{\xi} &= -\frac{1}{3\tilde{\varepsilon}} r + \frac{1+\tilde{\varepsilon}}{2\tilde{\varepsilon}} - \frac{(1-\tilde{\varepsilon})^3}{6\tilde{\varepsilon}} \frac{1}{r^2} + \frac{f}{Z} \quad \text{for} \quad 1 - \tilde{\varepsilon} < r < 1 + \tilde{\varepsilon}, \\
\overline{\xi} &= \frac{3+\tilde{\varepsilon}^2}{3} \frac{1}{r^2} + \frac{f}{Z} \quad \text{for} \quad 1 + \tilde{\varepsilon} < r < \infty, \\
\overline{\zeta}^a &= 1 + \frac{f}{Z} \quad \text{for} \quad 0 < r < 1 - \tilde{\varepsilon}, \\
\overline{\zeta}^a &= \frac{1+\tilde{\varepsilon}}{2\tilde{\varepsilon}} - \frac{1}{2\tilde{\varepsilon}} r + \frac{f}{Z} \quad \text{for} \quad 1 - \tilde{\varepsilon} < r < 1 + \tilde{\varepsilon}, \\
\overline{\zeta}^a &= \frac{f}{Z} \quad \text{for} \quad 1 + \tilde{\varepsilon} < r < \infty,
\end{aligned} \tag{38}
$$

where $\tilde{\varepsilon} = \varepsilon / R$.

The nondimensional linearized equations (16) with Eqs. (38) is numerically solved with the discretization in the radial direction, $0 = r_0 < r_1 < r_2 < \cdots < r_N < r_{N+1} < \infty$. The variables are radially discretized as

$$
\hat{a}(r_0, t) = \hat{a}_0(t),\ \hat{a}(r_1, t) = \hat{a}_1(t),\ \cdots,\ \hat{a}(r_N, t) = \hat{a}_N(t),\ \hat{a}(r_{N+1}, t) = \hat{a}_{N+1}(t), \tag{39}
$$

where $a = u,\ v$, or ϕ. The derivatives are so discretized that

$$
\left[\frac{\partial \hat{a}}{\partial r} \right]_{r=r_n} = \frac{\hat{a}_{n+1} - \hat{a}_{n-1}}{r_{n+1} - r_{n-1}} \quad \text{for} \quad 1 \le n \le N \quad \text{with} \ \ \hat{a}_0 = \hat{a}_{N+1} = 0, \tag{40}
$$

where $a = u$ or ϕ. We set $N = 100$ and discretize the radial direction so that the area of each annulus $r_{n-1} < r < r_n$ $(n = 1, 2, \cdots, N+1)$ is equal to one another. Specifically, we set $r_n = \sqrt{n/20}$ $(n = 0, 1, 2, \cdots, N, N+1)$ and $r_{20} = 1$ is the nondimensionalized Rankine radius. Substituting Eqs. (39)

and (40) into Eqs. (16) gives

$$\begin{aligned}
\frac{\partial \hat{u}_n}{\partial t} &= -im\overline{\omega}_n \hat{u}_n + \overline{\xi}_n \hat{v}_n - \frac{\hat{\phi}_{n+1} - \hat{\phi}_{n-1}}{r_{n+1} - r_{n-1}}, \\
\frac{\partial \hat{v}_n}{\partial t} &= -im\overline{\omega}_n \hat{v}_n - \overline{\zeta}^a_n \hat{u}_n - \frac{im}{r_n}\hat{\phi}_n, \\
\frac{\partial \hat{\phi}_n}{\partial t} &= -im\overline{\omega}_n \hat{\phi}_n - \gamma \left\{ \frac{\hat{u}_n}{r_n} + \frac{\hat{u}_{n+1} - \hat{u}_{n-1}}{r_{n+1} - r_{n-1}} + \frac{im}{r_n}\hat{v}_n \right\} \qquad \text{for} \quad 1 \le n \le N,
\end{aligned}$$

where $\overline{\omega}_n = \overline{\omega}(r_n)$ etc. These can be rewritten in the following vector form,

$$\frac{\partial}{\partial t}|\hat{U}(t)\rangle = A|U(t)\rangle, \tag{41}$$

where $|\hat{U}(t)\rangle$ is a $3N$ column vector and A is a $3N \times 3N$ matrix.

$$|\hat{U}(t)\rangle = \begin{bmatrix} \hat{u}_1(t) \\ \hat{v}_1(t) \\ \hat{\phi}_1(t) \\ . \\ . \\ . \\ \hat{u}_N(t) \\ \hat{v}_N(t) \\ \hat{\phi}_N(t) \end{bmatrix} \quad \text{and} \quad A = \begin{bmatrix} B_1 & -C_1 & 0 & 0 & 0 & \cdots & 0 \\ C_2 & B_2 & -C_2 & 0 & 0 & \cdots & 0 \\ 0 & C_3 & B_3 & -C_3 & 0 & \cdots & 0 \\ & & \cdots & & & & \\ & & & \cdots & & & \\ & & & & \cdots & & \\ 0 & \cdots & 0 & C_{N-2} & B_{N-2} & -C_{N-2} & 0 \\ 0 & \cdots & 0 & 0 & C_{N-1} & B_{N-1} & -C_{N-1} \\ 0 & \cdots & 0 & 0 & 0 & C_N & B_N \end{bmatrix} \tag{42}$$

where

$$B_n = \begin{bmatrix} -im\overline{\omega}_n & \overline{\xi}_n & 0 \\ -\overline{\zeta}^a_n & -im\overline{\omega}_n & -im/r_n \\ -\gamma/r_n & -i\gamma m/r_n & -im\overline{\omega}_n \end{bmatrix} \text{ and } C_n = \begin{bmatrix} 0 & 0 & 1/(r_{n+1}-r_{n-1}) \\ 0 & 0 & 0 \\ \gamma/(r_{n+1}-r_{n-1}) & 0 & 0 \end{bmatrix}.$$

The solution to Eq. (41) with an initial values $|\hat{U}(0)\rangle$ is given by

$$|\hat{U}(t)\rangle = \sum_{n=1}^{3N} e^{\lambda_n t} \frac{|R_n\rangle\langle L_n|}{\langle L_n|R_n\rangle} |\hat{U}(0)\rangle, \tag{43}$$

where λ_n $(n = 1, 2, \cdots, 3N)$ are the eigenvalues of the matrix A in Eqs. (42), and $|R_n\rangle$ and $\langle L_n|$ are the corresponding right and left eigenvectors, respectively. The right and left eigenvectors are $3N$ column and $3N$ row vectors, respectively. The dyadic product $|R_n\rangle\langle L_n|$ in the numerator on the RHS of Eq. (43) is a $3N \times 3N$ matrix, and the inner product $\langle L_n|R_n\rangle$ in the denominator is a scalar. By the definition of the eigenvalues and right eigenvectors $A|R_n\rangle = \lambda_n|R_n\rangle$ $(n = 1, 2, \cdots, 3N)$, and by the completeness relation of the right and left eigenvectors $\sum_{n=1}^{3N} |R_n\rangle\langle L_n|/\langle L_n|R_n\rangle = I_{3N}$(which is an identity matrix), we can easily see that the expression in Eq. (43) is indeed the solution to Eq. (41) with the prescribed initial value $|\hat{U}(0)\rangle$.

$$\frac{\partial}{\partial t} \sum_{n=1}^{3N} e^{\lambda_n t} \frac{|R_n\rangle\langle L_n|}{\langle L_n|R_n\rangle} |\hat{U}(0)\rangle = \sum_{n=1}^{3N} e^{\lambda_n t} \lambda_n \frac{|R_n\rangle\langle L_n|}{\langle L_n|R_n\rangle} |\hat{U}(0)\rangle = A \sum_{n=1}^{3N} e^{\lambda_n t} \frac{|R_n\rangle\langle L_n|}{\langle L_n|R_n\rangle} |\hat{U}(0)\rangle,$$
$$\left[\sum_{n=1}^{3N} e^{\lambda_n t} \frac{|R_n\rangle\langle L_n|}{\langle L_n|R_n\rangle} |\hat{U}(0)\rangle \right]_{t=0} = \sum_{n=1}^{3N} \frac{|R_n\rangle\langle L_n|}{\langle L_n|R_n\rangle} |\hat{U}(0)\rangle = |\hat{U}(0)\rangle.$$

The solution to Eq. (41) with an initial value $|\hat{U}(0)\rangle$ is also written as

$$|\hat{U}(t)\rangle = e^{At}|\hat{U}(0)\rangle = \sum_{n=0}^{\infty} \frac{t^n}{n!} A^n |\hat{U}(0)\rangle. \tag{44}$$

We can also easily see that the expression in Eq. (44) is indeed the solution to Eq. (41) with the prescribed initial value $|\hat{U}(0)\rangle$.

$$\frac{\partial}{\partial t} \sum_{n=0}^{\infty} \frac{t^n}{n!} A^n |\hat{U}(0)\rangle = \sum_{n=1}^{\infty} \frac{t^{n-1}}{(n-1)!} A^n |\hat{U}(0)\rangle = A \sum_{n=0}^{\infty} \frac{t^n}{n!} A^n |\hat{U}(0)\rangle,$$

$$\left[\sum_{n=0}^{\infty} \frac{t^n}{n!} A^n |\hat{U}(0)\rangle \right]_{t=0} = \sum_{n=0}^{\infty} \frac{0^n}{n!} A^n |\hat{U}(0)\rangle = |\hat{U}(0)\rangle.$$

The equivalence of the expressions Eqs. (43) and (44) is easily checked by the use of the spectral decomposition of A and the orthogonality of $\langle L_n|$ and $|R_n\rangle$,

$$A = \sum_{n=1}^{3N} \lambda_n \frac{|R_n\rangle\langle L_n|}{\langle L_n|R_n\rangle} \quad \text{and} \quad \langle L_n|R_m\rangle = 0 \ \text{ if } \ n \neq m.$$

For growing solutions to exist, there must exist at least one eigenvalue with positive real part.

Let λ_M be the eigenvalue with the largest positive real part, and $|R_M\rangle$ and $\langle L_M|$ be the corresponding right and left eigenvectors, respectively. Then, as $t \to \infty$, the term of λ_M in Eq. (43) becomes dominant,

$$\lim_{t\to\infty} |\hat{U}(t)\rangle \sim e^{\lambda_M t} \frac{|R_M\rangle\langle L_M|}{\langle L_M|R_M\rangle} |\hat{U}(0)\rangle = e^{\lambda_M t} \frac{\langle L_M|\hat{U}(0)\rangle}{\langle L_M|R_M\rangle} |R_M\rangle \propto e^{\lambda_M t}|R_M\rangle.$$

The spatial structure and temporal evolution of the growing disturbance is determined by $e^{\lambda_M t}|R_M\rangle$. Since the disturbance in the physical space is given by Eqs. (8), the structure, the growth rate, and angular phase velocity of the growing eigen-disturbance are respectively given by,

$$\text{the structure} = \mathrm{Re}\left[e^{im\theta}|R_M\rangle\right]\cos\pi z \qquad \text{(after nondimensionalization } z \to Hz\text{)}, \tag{45}$$

$$\text{the growth rate} = \mathrm{Re}\left[\lambda_M\right], \tag{46}$$

$$\text{the angular phase velocity} = -\frac{1}{m}\mathrm{Im}\left[\lambda_M\right]. \tag{47}$$

The eigenvalue λ_M and right eigenvector $|R_M\rangle$ are numerically calculated. In the calculation, in order to suppress reflection, the variables are forced to linearly decrease to zero near the lateral boundary. The structure of the growing eigen-disturbance given by Eq. (45) with azimuthal wave number $m = 2$ is shown in Fig. 7, which is so displayed as to correspond to Fig. 6 of the conceptual model in subsection 2.4. The value of the first parameter f/Z is so set $f/Z = 0.02$ as stated at the end of subsection 3.1. The value of the second parameter γ is so set $\gamma = 0.006$ that the growth rate (i.e., the value of $\mathrm{Re}[\lambda_M]$) becomes maximum in the range of $0 < \gamma < 0.02$ for the fixed $f/Z = 0.02$. Fig. 7

In Fig. 7, the disturbance buoyancy $b = \partial\phi/\partial z$ is shown instead of ϕ. The disturbance $\hat{b}$ in the mode assumed in Eqs. (8) is related to $\hat{\phi}$ as $\hat{b} = -\hat{\phi}$ after the nondimensionalization in Eqs. (14), and $z \to Hz$ and $\hat{b} \to [\hat{b}]\hat{b}$ with $[\hat{b}] = (\pi/H)[\hat{\phi}]$. Further, in order to display the VRW, the disturbance potential vorticity q is shown instead of the disturbance vertical vorticity ζ. The disturbance $\hat{q}$ in the mode assumed in Eqs. (8) is related to $\hat{\zeta}$ as $\hat{q} = \gamma\hat{\zeta} - \overline{\zeta}^a\hat{\phi}$ after the nondimensionalization in Eqs. (14) and (38). The reason of the preference for q than ζ is that another ζ perturbation associated with the GW is also present away from the Rankine radius in addition to the ζ perturbation associated with the VRW at (and near) the Rankine radius. From Eq. (29), the GW is necessarily accompanied with the vertical vorticity perturbation.

The disturbance potential vorticity q in (a) and (c) of Fig. 7, and the outer horizontal divergence $HD_{\rm out}$ in (a) and (c), and outer buoyancy $b_{\rm out}$ in (b), which are located outside of the Rankine radius, are so structured as to be compatible with the conceptual model of VRW-GW interaction depicted in Figs. 4, 5, and 6. That is, q and $HD_{\rm out}$ on $z = 0, 1$ are phase-locked with a phase difference π, and $HD_{\rm out}$ on $z = 0 (z = 1)$ is located one quarter wave length downstream (upstream) of $b_{\rm out}$ on $z = 1/2$.

In addition to the outer perturbations $HD_{\rm out}$ and $b_{\rm out}$, there exist also other inner perturbations $HD_{\rm in}$ and $b_{\rm in}$ in Fig. 7, which are located in the vicinity of the Rankine radius. From Eq. (32), the exponential growth of ζ at the Rankine radius (i.e., the growth of VRW) is necessarily accompanied with the exponential growth of $\phi_{\rm in}$ there, and so the exponential growth of $b_{\rm in} = \partial\phi_{\rm in}/\partial z$ there. For $b_{\rm in}$ to be part of the form-preserving eigen-disturbance, there must exist also HD_{in} to form an azimuthally propagating GW_{in}. The GW_{in} propagates anticyclonically and is strongly advected cyclonically by the basic vortex so that it becomes part of the form-preserving eigen-disturbance slowly moving cyclonically. Indeed, the anticyclonic propagation of the GW_{in} is seen in Fig. 7. That is, HD_{in} on $z = 0$ ($z = 1$) lies one quarter wave length upstream (downstream) of b_{in} on $z = 1/2$.

The numerically calculated growth rate in Eq. (46) and the angular phase velocity in Eq. (47) of the growing eigen-disturbance are $\text{Re}\,[\lambda_M] \approx 0.05$ and $-(1/2)\text{Im}\,[\lambda_M] \approx 0.34$, respectively. The growth rate is small compared with the growth rate and angular phase velocity of the growing disturbance due to the VRW-VRW interaction which are $O(1)$ or $O(Z)$ s^{-1} in the dimensional units.

5. Concluding remarks

In this paper, we proposed a simple conceptual model of the resonant interaction between the VRW and GW on a typhoon-like basic vortex. Further, we analytically showed the possibility of the interaction, and numerically obtained the growing solution in the system linearized about the basic vortex.

In order to make the problem simplest and to grasp the essential mechanism, although the reality is rather complicated and intricate, the basic vortex was assumed to be a stably stratified barotropic Rankine vortex, and the disturbance on the vortex was assumed to be of the first baroclinic vertical mode and of the azimuthal wave number $m \neq 0$ mode.

The central VRW, which is located at the jump radius of the Rankine vortex, moves cyclonically because of the strong cyclonic advection by the basic vortex flow and weak anticyclonic propagation ("propagation" means "propagation relative to the fluid") due to the radial inward gradient of the basic vertical vorticity. The outer GW, which is assumed to be located outside of the jump radius of the Rankine vortex, moves also cyclonically because of the weak cyclonic advection by the basic vortex flow and cyclonic propagation due to the stable stratification. The VRW and GW are counter-propagating to each other, and therefore satisfy Rayleigh's condition for instability. Further, both of them move cyclonically, and therefore may satisfy Fjørtoft's condition for instability, that is, may be phase-locked with each other. If the counter-propagating VRW and GW become phase-locked, they resonantly interact with each other and grow. We assumed the existence of such an outer GW that can be phase-locked with the central VRW, and we considered the resonant interaction between them based on the BV-thinking.

As is already known, the resonant interaction between RWs (or vorticity waves in general) and GWs (i.e., buoyancy waves) in a vertical-zonal system is conceptually clearly grasped based on the BV-thinking (e.g., Carpenter et al. 2011). The RW in the 2-dimensional system is a horizontal vorticity wave and is accompanied with vertical circulation. The GW in the 2-dimensional system is a buoyancy wave and is also accompanied with vertical circulation. In the resonant interaction between them, the vertical circulation of RW amplifies the GW, and simultaneously the vertical circulation of GW amplifies the RW, resulting in the resonant growth. On the other hand, the VRW and GW of the present problem interact with each other in a 3-dimensional system. As in the vertical-zonal 2-dimensional problem, the GW is a buoyancy wave, and is accompanied with vertical circulation. However, different from the vertical-zonal 2-dimensional problem, the VRW in the 3-dimensional system is a vertical vorticity wave, and is accompanied with horizontal circulation. Although the 3-dimensional resonant interaction including vertical and horizontal circulations cannot be understood as a straightforward extension of the 2-dimensional resonant interaction including only vertical circulations, it can be also conceptually grasped based on the BV-thinking as presented in Section 2. That is, the horizontal circulation of VRW amplifies the GW, and simultaneously the vertical circulation of GW amplifies the VRW. Specifically, in the proposed conceptual model presented in Section 2, the central VRW, whose amplitude is maximum on the lower and upper levels, is expressed in terms of the disturbance vertical vorticity ζ. The horizontal circulation around ζ advects the basic vertical vorticity $\bar{\zeta}$ and generates new ζ. The successive generation of ζ makes the VRW propagate anticyclonically. The outer GW, whose amplitude is maximum on the middle level, is expressed in terms of the disturbance radial vorticity η and the disturbance buoyancy b. The vertical circulation around η advects the basic buoyancy $\bar{b}$ (that is, the basic potential temperature) and generates new b. At the same time, the azimuthal gradient of b generates new η. The successive mutual generation of η and b makes the GW propagate cyclonically. On the assumption of phase-lock, the horizontal circulation around ζ induces vertical circulation in the outer region which advects $\bar{b}$ and enhances b. At the same time, the vertical circulation around η induces horizontal circulation in the central region which advects $\bar{\zeta}$ and enhances ζ. As a result, the VRW and GW resonantly grow.

We analytically examined the system of equations linearized about the basic vortex, and showed the possibility of the resonant interaction. The VRW in the central region and the GW in the outer region may reinforce each other. Further, we numerically obtained the growing solution of the linearized system. The growing solution shows the resonant interaction structure proposed in the conceptual model, although the growth rate is rather small.

Because of the smallness of the growth rate, the VRW-GW interaction does not come into question in the presence of the VRW-VRW interaction. For a typhoon-like vortex with an annulus of high vertical vorticity corresponding to the eyewall and/or with an annulus of low vertical vorticity in the outer region, Rayleigh's condition for instability of the VRW-VRW interaction is satisfied, and VRWs grow by the interaction. The growing VRWs near the eyewall are supposed to be related with the eye deformation and the track meandering. While, those near the outer annulus of low vertical vorticity are supposed to be related with the eye replacement cycle. In these cases, the VRW-GW interaction, which may exist, has little contribution to the growth of VRWs. On the other hand, in the case of a monopolar vortex, the radial gradient of the basic vertical vorticity is everywhere negative, and therefore Rayleigh's condition for instability of the VRW-VRW interaction is not satisfied. As a result, VRWs cannot grow by the interaction. However, VRWs can still grow by the VRW-GW interaction even for a monopolar vortex. The growing VRWs by VRW-GW interaction may play the role of those by VRW-VRW interaction, instead.

The growing eigen-disturbance in our numerical calculation has an inner GW in addition to the outer GW which resonantly interacts with the central VRW. Although the inner GW propagates anticyclonically, it is advected cyclonically by the strong basic angular velocity, and moves cyclonically.

Because of the cyclonic movement, the inner GW is phase-locked with the outer GW which moves also cyclonically, and the two GWs constitute the form-preserving eigen-disturbance. The inner and outer GWs propagate anticyclonically and cyclonically, respectively, that is, are counter-propagating to each other, and therefore they satisfy Rayleigh's condition for instability. The two GWs satisfying Rayleigh's condition are phase-locked with each other. Hence, the interaction between them (GW-GW interaction) may contributes to the growth of the eigen-disturbance. If so, what growing mechanism the GW-GW interaction has, and what relation the GW-GW interaction has to the VRW-GW interaction? To examine these, it belong to our future study.

The inner GW of the numerically calculated growing eigen-disturbance is colocated and comoving with the VRW in the vicinity of the Rankine radius. The pair of VRW and GW is reminiscent of the mixed vortex Rossby-gravity wave of Zhong et al. (2009). To examine whether they have any relation or not, it belongs also to our future study.

References

Bretherton, F. P., 1966: Baroclinic instability and the short wavelength cut-off in terms of potential vorticity. Quart.J.Roy.Meteor.Soc., **92**, 335–345.

Cairns, R. A., 1979: The role of negative energy waves in some instabilities of parallel flows. J.Fluid.Mech., **92**, 1–14.

Carpenter, J. R., E. W. Tedford, E. Heifetz, and L. G. A, 2011: Instability in stratified shear flow: Review of a physical interpretation based on interacting waves. Applied Mechanics Reviews, **64**, 061001 1–17.

Harnik, N., E. Heifetz, O. M. Umurhan, and F. Lott, 2008: A buoyancy-vorticity wave interaction approach to stratified shear flow. J.Atmos.Sci., **65**, 2615–2630.

Heifetz, E., C. H. Bishop, and P. Alpert, 1999: Counter-propagating Rossby waves in the barotropic Rayleigh model of shear instability. Quart.J.Roy.Meteor.Soc., **125**, 2835–2853.

Hodyss, D., and D. S. Nolan, 2008: The Rossby-inertia-buoyancy instability in baroclinic vortices. Phys.Fluids, **20**, 096602 1–21.

Hoskins, B. J., M. E. McIntyre, and A. W. Robertson, 1985: On the use and significance of isentropic potential vorticity maps. Quart.J.Roy.Meteor.Soc., **111**, 877–946.

Kossin, J. P., and W. H. Schubert, 2001: Mesovortices, polygonal flow patterns, and rapid pressure falls in hurricane-like vortices. J.Atmos.Sci., **58**, 2196–2209.

Kossin, J. P., and W. H. Schubert, 2004: Mesovortices in hurricane Isabel. Bull.Amer.Meteor.Soc., **85**, 151–153.

Menelaou, K., D. A. Schecter, and M. K. Yau, 2016: On the relative contribution of inertia-gravity wave radiation to asymmetric instabilities in tropical cyclone-like vortices. J.Atmos.Sci., **73**, 3345–3370.

Montgomery, M. T., and R. J. Kallenbach, 1997: A theory for vortex Rossby waves and its application to spiral bands and intensity changes in hurricanes. Quart.J.Roy.Meteor.Soc., **123**, 435–465.

Nolan, D. S., and M. T. Montgomery, 2000: The algebraic growth of wavenumber one disturbances in hurricane-like vortices. J.Atmos.Sci., **57**, 3514–3538.

Nolan, D. S., and M. T. Montgomery, 2002: Nonhydrostatic, three-dimensional perturbations to balanced hurricane-like vortices. partI : Linearized formulation, stability, and evolution. J.Atmos.Sci., **59**, 2989–3020.

Nolan, D. S., M. T. Montgomery, and L. D. Grasso, 2001: The wavenumber-one instability and trochoidal motion of hurricane-like vortices. J.Atmos.Sci., **58**, 3243–3270.

Rabinovich, A., O. M. Umurhan, N. Harnik, F. Lott, and E. Heifetz, 2011: Vorticity inversion and action-at-a-distance instability in stably stratified shear flow. J.Fluid Mech, **670**, 301–325.

Sakai, S., 1989: Rossby-kelvin instability : a new type of ageostophic instability caused by a resonance between rossby waves and gravity waves. J.Fluid.Mech., **202**, 140–176.

Schecter, D. A., and M. T. Montgomery, 2004: Damping and pumping of a vortex Rossby wave in a monotonic cyclone: Critical layer stirring versus inertia-buoyancy wave emission. Phys.Fluids, **16**, 1334–1348.

Schecter, D. A., and M. T. Montgomery, 2006: Conditions that inhibit the spontaneous radiation of spiral inertia-gravity waves from an intense mesoscale cyclone. J.Atmos.Sci., **63**, 435–456.

Schecter, D. A., M. T. Montgomery, and P. D. Reasor, 2002: A theory for the vertical alignment of a quasigeostrophic vortex. J.Atmos.Sci., **59**, 150–168.

Schubert, W. H., M. T. Montgomery, R. K. Taft, T. A. Guinn, S. R. Fulton, J. P. Kossin, and J. P. Edwards, 1999: Polygonal eyewalls, asymmetric eye contraction, and potential vorticity mixing in hurricanes. J.Atoms.Sci., **56**, 1197–1223.

Willoughby, H. E., 1977: Inertia-buoyancy waves in hurricanes. J.Atmos.Sci., **34**, 1028–1039.

Willoughby, H. E., 1978: A possible mechanism for the formation of hurricane rainbands. J.Atmos.Sci., **35**, 838–848.

Zhong, W., D. Zhang, and H. Lu, 2009: A theory for mixed vortex Rossby-gravity waves in tropical cyclones. J.Atmos.Sci., **66**, 3366–3381.

List of Figures

1 Stably stratified barotropic Rankine vortex. $\bar{\zeta}$ is the basic vertical vorticity. $\bar{b}$ is the basic buoyancy. 51

2 Propagation of VRW at $r = R$. The black curves are the Iso-$(\bar{\zeta} + \zeta)$ lines. The black arrows $\uparrow\downarrow\uparrow$ represent the horizontal circulations induced by the vertical vorticity perturbation ζ. 52

3 Propagation of GW at $r = \tilde{R}$. The black curves are the Iso-$(\bar{b} + b)$ lines. The red circles with arrows represent the radial vorticity perturbation η. The red arrows $\downarrow\uparrow\downarrow$ represent the vertical circulations induced by η. The black arrows $\uparrow\downarrow$ represent the buoyancy force caused by b. 53

4 Interaction between VRW at $r = R$ and GW at $r = \tilde{R}$ $(> R)$. The black curves in the top and bottom are the Iso-$(\bar{\zeta} + \zeta)$ lines. The black curve in the middle is the Iso-$(\bar{b} + b)$ line. The red circles with arrows in the middle represent the radial vorticity perturbations η. The black arrows $\uparrow\downarrow\uparrow$ in the top and bottom represent the horizontal circulations induced by the vertical vorticity perturbations ζ. The red arrows $\downarrow\uparrow\downarrow$ in the middle represent the vertical circulations induced by η. The black circles with VD and VC respectively represent the vertical divergence and convergence generated by the horizontal circulations. The red circles with HD and HC respectively represent the horizontal divergence and convergence generated by the vertical circulations. The red short uparrows $\Uparrow$ and downarrows $\Downarrow$ represent the amplification of VRW by GW. The black short uparrow $\Uparrow$ and downarrow $\Downarrow$ represent the amplification of GW by VRW. 54

5 Three-dimensional view of Fig 4. 55

6 Plan views of Fig 4on $z = 1$(a), $z = 1/2$(b), and $z = 0$(c). . 56

7 Structure of growing eigen-disturbance corresponding to the eigenvalue λ_M with the largest real part. The parameter values are set $f/Z = 0.02$, $\gamma = 0.006$, and $m = 2$. Only the inside of twice the Rankine radius is shown. (a) The disturbance potential vorticity q(left) and disturbance horizontal divergence HD (right) on $z = 1$. (b) The disturbance vertical velocity w (left) and buoyancy b (right) on $z = 1/2$. (c) The disturbance potential vorticity q (left) and disturbance horizontal divergence HD (right) on $z = 0$. 57

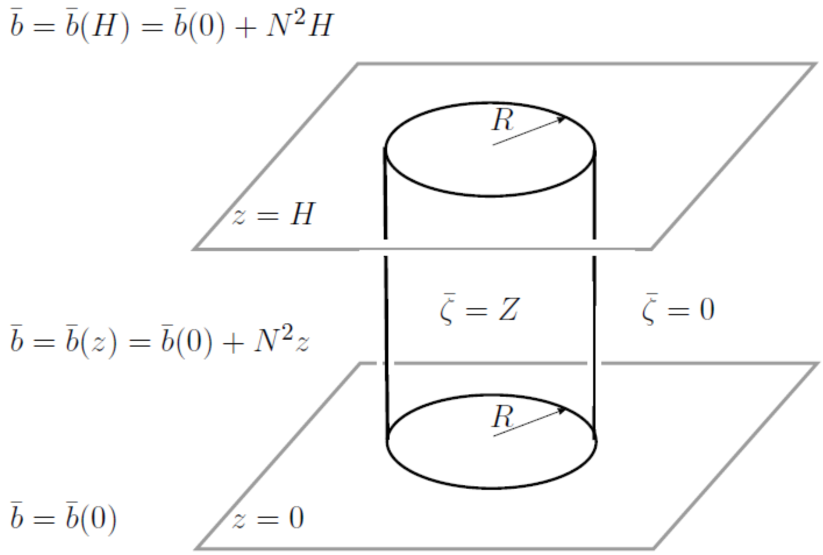

Fig. 1. Stably stratified barotropic Rankine vortex. $\overline{\zeta}$ is the basic vertical vorticity. $\overline{b}$ is the basic buoyancy.

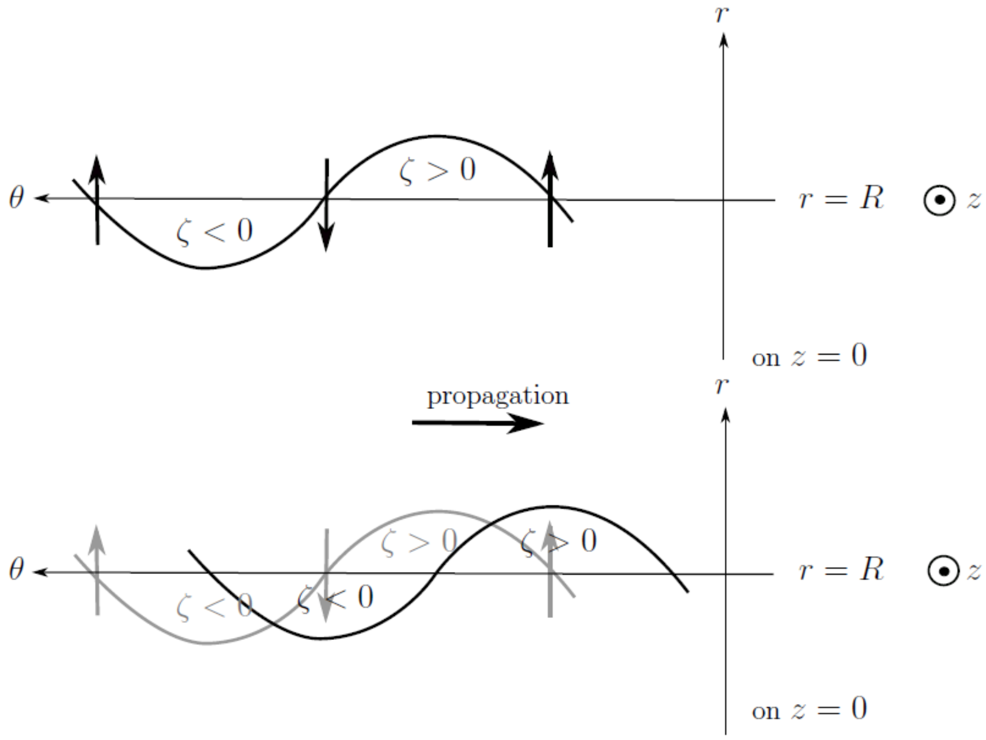

Fig. 2. Propagation of VRW at $r = R$. The black curves are the Iso-$(\bar{\zeta}+\zeta)$ lines. The black arrows ↑↓↑ represent the horizontal circulations induced by the vertical vorticity perturbation ζ.

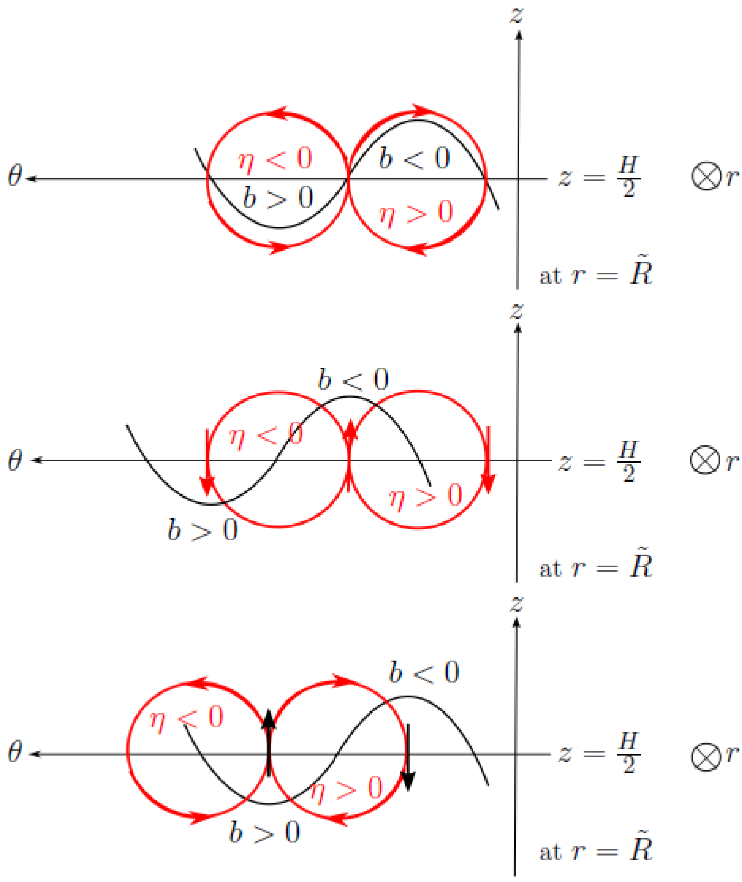

Fig. 3. Propagation of GW at $r = \tilde{R}$. The black curves are the Iso-$(\bar{b}+b)$ lines. The red circles with arrows represent the radial vorticity perturbation η. The red arrows ↓↑↓ represent the vertical circulations induced by η. The black arrows ↑↓ represent the buoyancy force caused by b.

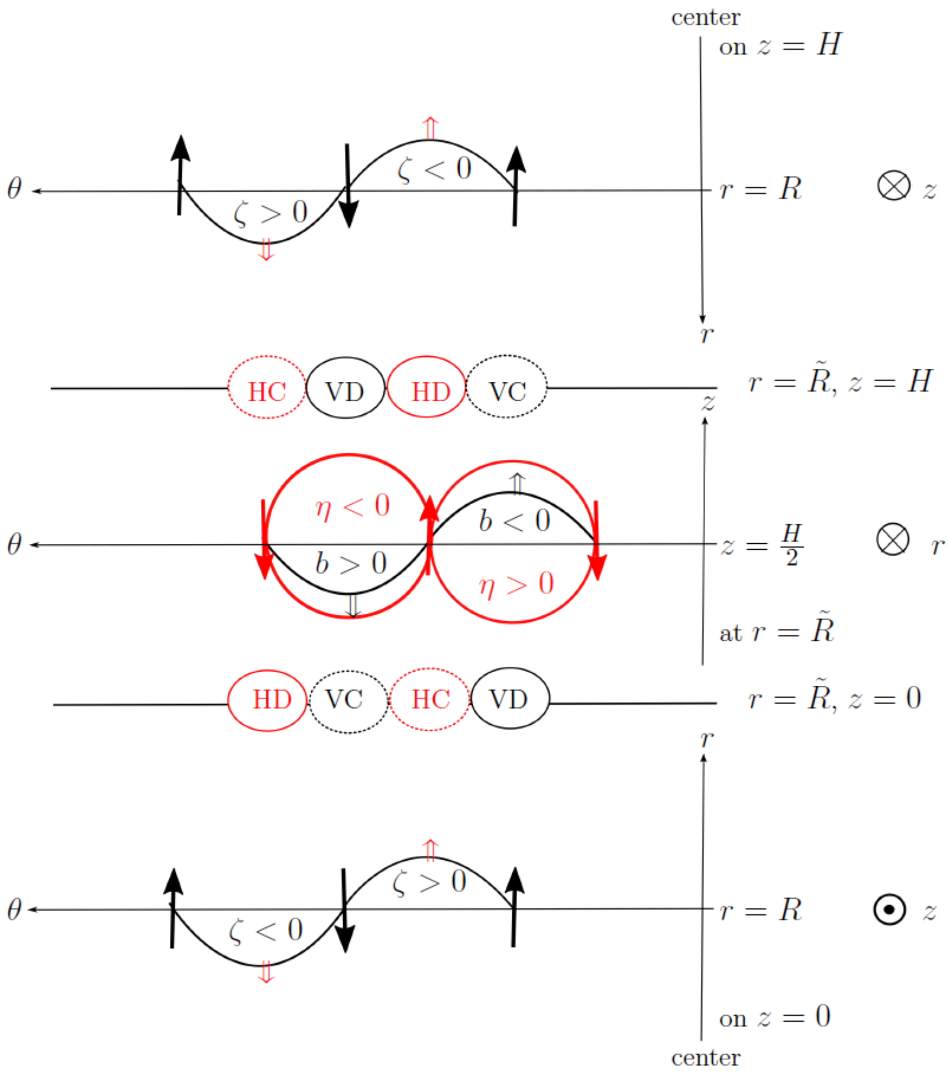

Fig. 4. Interaction between VRW at $r=R$ and GW at $r=\tilde{R}$ ($>R$). The black curves in the top and bottom are the Iso-($\overline{\zeta}+\zeta$) lines. The black curve in the middle is the Iso-($\overline{b}+b$) line. The red circles with arrows in the middle represent the radial vorticity perturbations η. The black arrows $\uparrow\downarrow\uparrow$ in the top and bottom represent the horizontal circulations induced by the vertical vorticity perturbations ζ. The red arrows $\downarrow\uparrow\downarrow$ in the middle represent the vertical circulations induced by η. The black circles with VD and VC respectively represent the vertical divergence and convergence generated by the horizontal circulations. The red circles with HD and HC respectively represent the horizontal divergence and convergence generated by the vertical circulations. The red short uparrows $\Uparrow$ and downarrows $\Downarrow$ represent the amplification of VRW by GW. The black short uparrow $\Uparrow$ and downarrow $\Downarrow$ represent the amplification of GW by VRW.

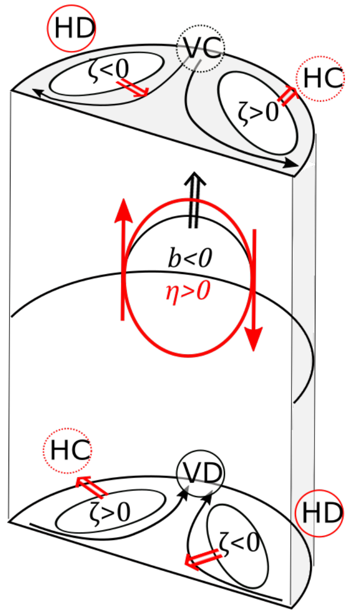

Fig. 5. Three-dimensional view of Fig 4.

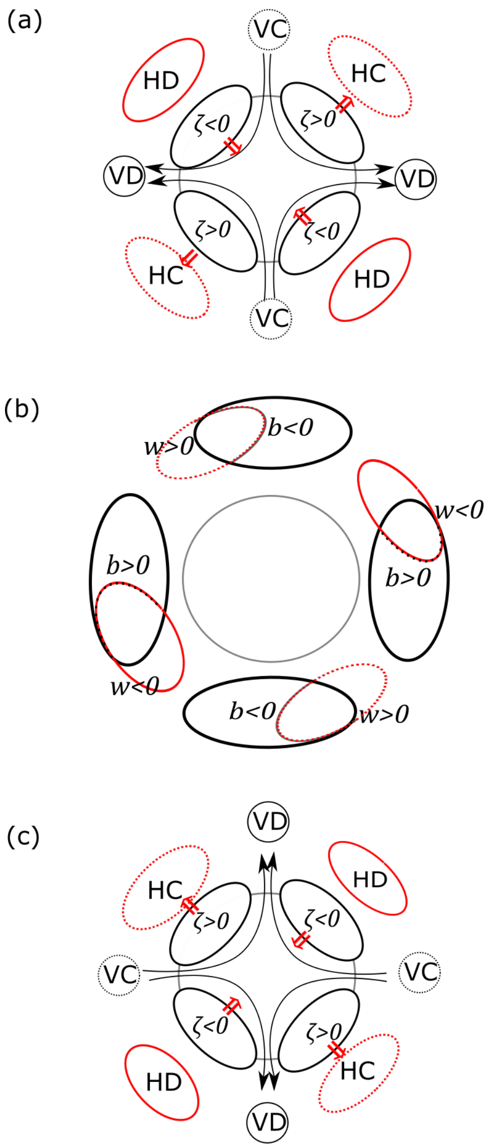

Fig. 6. Plan views of Fig 4 on $z = 1$(a), $z = 1/2$(b), and $z = 0$(c).

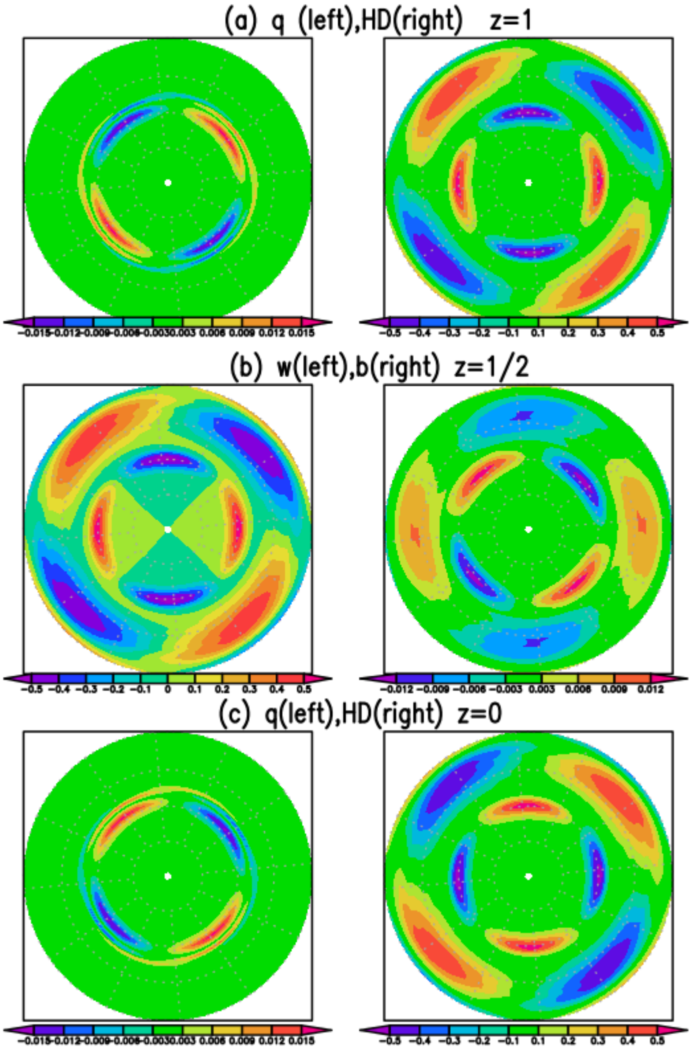

Fig. 7. Structure of growing eigen-disturbance corresponding to the eigenvalue λ_M with the largest real part. The parameter values are set $f/Z = 0.02$, $\gamma = 0.006$, and $m = 2$. Only the inside of twice the Rankine radius is shown. (a) The disturbance potential vorticity q(left) and disturbance horizontal divergence HD (right) on $z = 1$. (b) The disturbance vertical velocity w (left) and buoyancy b (right) on $z = 1/2$. (c) The disturbance potential vorticity q (left) and disturbance horizontal divergence HD (right) on $z = 0$.